Probing heterogeneous dynamics of a repulsive colloidal glass by time resolved x-ray correlation spectroscopy

2008 J. Phys.: Condens. Matter 20 155104

(http://iopscience.iop.org/0953-8984/20/15/155104)

IOP PUBLISHING JOURNAL OF PHYSICS: CONDENSED MATTER

J. Phys.: Condens. Matter **20** (2008) 155104 (7pp) doi:10.1088/0953-8984/20/15/155104

Probing heterogeneous dynamics of a repulsive colloidal glass by time resolved x-ray correlation spectroscopy

E Wandersman[1], A Duri[2], A Robert[3,4], E Dubois[1], V Dupuis[1] and R Perzynski[1]

[1] Laboratoire des Liquides Ioniques et Interfaces chargées, UMR 7612, Université Paris VI-CNRS, 4, Place Jussieu 75005, Paris, France
[2] Deutsches Elektronen-Synchrotron (Hasylab), Notkestraße 85-22607 Hamburg, Germany
[3] European Synchrotron Radiation Facility, 6 rue J. Horowitz BP 220, 38043 Grenoble Cedex 9, France
[4] Stanford Linear Accelerator Center, Stanford University LUSI/LCLS, 2575 Sand Hill road, MS 43A, Menlo Park, CA 94025, USA

E-mail: wanders@ccr.jussieu.fr

Received 23 November 2007, in final form 5 February 2008
Published 10 March 2008
Online at stacks.iop.org/JPhysCM/20/155104

Abstract
We present here experimental results obtained by time resolved x-ray correlation spectroscopy, revealing the heterogeneous nature of the dynamics down to the nanoscale in a dense dispersion of magnetic nanoparticles. The dynamical susceptibility, which quantifies the amplitude of the dynamical fluctuations, is investigated in a repulsive colloidal glass. Its value is an order of magnitude smaller than the ones found in gels and is length scale independent in the Q-range of the x-ray scattering experiment.

(Some figures in this article are in colour only in the electronic version)

1. Introduction

A unified and complete understanding of the drastic dynamical slowing down observed at the glass transition in numerous disordered systems (molecular and colloidal glasses, fractal gels, spin glasses and granular materials . . .) remains a challenging question in statistical physics. Several conceptual and theoretical breakthroughs have revealed a formal similitude of all these glass transitions: the mode coupling theory (MCT) [1] predicts both in molecular and colloidal glasses a divergence of the characteristic times at a critical temperature (for molecular systems) or at a volume fraction (for colloidal systems). The concept of 'jamming' introduced by Liu and Nagel [2], has extended the universal character of these phenomena, for example to granular matter. Moreover, formal analogies have been uncovered [3] between the MCT and dynamical equations of spin glasses.

However, despite this generic behavior of the dynamical slowing down in various glassy systems, its physical origin is still not well understood and is widely debated. Some research relate this behavior to a growth of dynamically correlated domains inside which the particles move in a cooperative way [4, 5]. As the glass transition is approached, the number of cooperative regions decreases, leading to large fluctuations of the dynamics.

Recently, Berthier *et al* have demonstrated, both numerically and theoretically [6] that four-point correlators (two-point in time, two-point in space) are relevant quantities to enlighten the existence of dynamical heterogeneities. In a numerical simulation of a Lennard-Jones glass, they compute the dynamical susceptibility (the volume integral of the four-point correlator, see [6]) and show that this quantity is indeed increasing when approaching the glass transition [7].

From the experimental point of view, soft glassy matter (colloidal glasses, gels, micellar solutions etc, for a review see [8]) constitutes a model system to investigate the dynamical nature of the glass transition. Indeed, the large intrinsic sizes of these systems shift their characteristic relaxation times to experimentally accessible temporal and spatial length scales (e.g. with confocal microscopy [9] or dynamic light

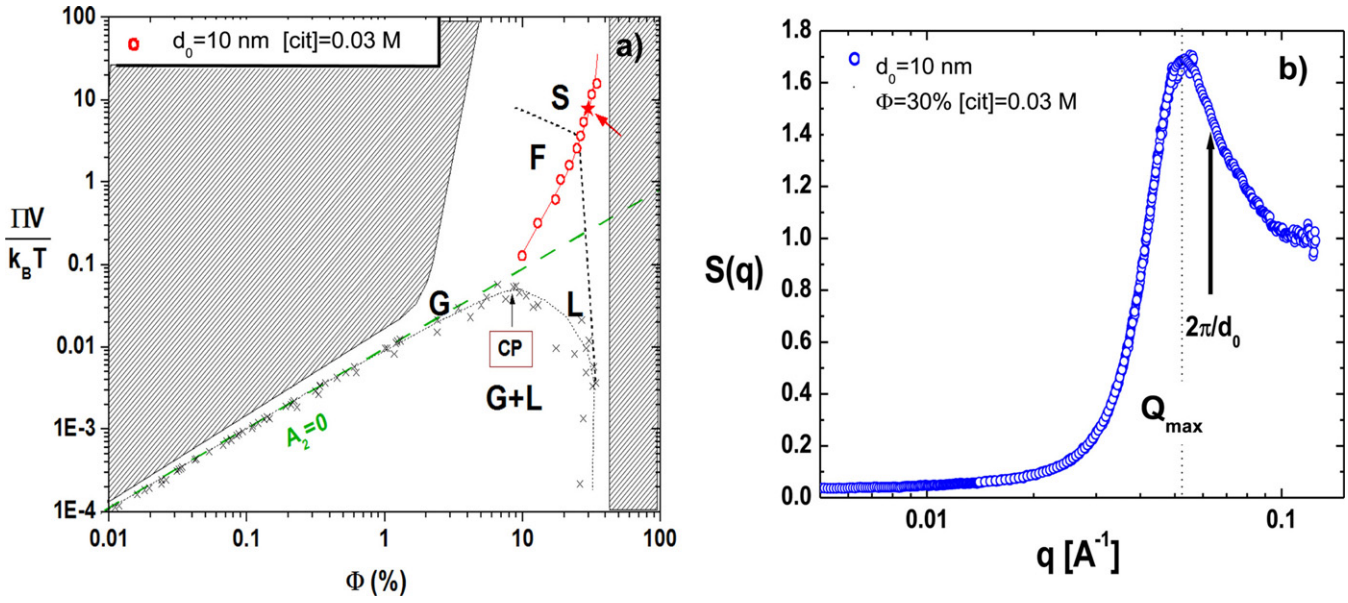

Figure 1. (a) Colloidal phase diagram in the osmotic pressure–volume fraction plane. Phases (G) = gas; (L) = liquid; (F) = fluid; (S) = solid, (CP) = critical point. Dashed black lines are guides delimiting different phases. The green dashed line is the 'perfect gas' line, corresponding to a null value of the second virial coefficient A_2. Open circles correspond to the samples at various Φ and [cit] = 0.03 mol l^{-1} (see [17]) and the solid star corresponds to the sample used for the XPCS experiment. (b) Static structure factor of the concentrated ferrofluid associated with the solid star in graphic (a) obtained by small angle x-ray scattering (SAXS) performed at the ID02 beamline of ESRF. The dotted line indicates the scattering vector Q_{max} associated with the maximum of the structure factor. The wavevector $2\pi/d_0$ corresponding to the contact between nanoparticles is indicated by an arrow.

scattering (DLS) [10, 11]), in comparison to molecular glasses. Recent developments of DLS by Cipelletti *et al* [10, 11], referred as 'multispeckle' detection and time resolved correlation (TRC) analysis, have allowed them to measure the aforementioned dynamical susceptibility and to quantify its spatial distribution [11]. However, discussions on this spatial distribution are still open and the studied systems exclusively concern gels or attractive systems, where heterogeneous dynamics is related to cluster rearrangements. To our knowledge, there is a lack of results concerning repulsive colloidal glasses, especially on the nanoscale, where the slowing down of the dynamics is potentially due to caging effects and not to the formation of large structures in the dispersion.

We will focus here on the investigation of dynamical heterogeneities in a repulsive colloidal glass, using a concentrated dispersion of magnetic nanoparticles (i.e. a concentrated ferrofluid), which are interacting with a strong repulsive potential. As the experiments are performed in the absence of an external magnetic field, the magnetic character of the ferrofluid is irrelevant here. The present paper is organized as follows: we first present properties of ferrofluids and show that the concentrated dispersions used in this study are repulsive colloidal glasses, according to [12]. We then show that x-ray photon correlation spectroscopy (XPCS) allows us to investigate the slow dynamics of the nanoparticles and to characterize its aging behavior down to the nanoscale. We then investigate the temporal heterogeneities of the dynamics using TRC analysis and present the measured dynamical susceptibility of this repulsive glass. Their dependence with regard to the probed length scales is considered. Finally we discuss and compare the experimental results obtained with this repulsive glass and those from the literature, obtained with gels [11, 13], granular matter [5, 14] or other glass formers [4].

2. The concentrated ferrofluids

2.1. Ionic ferrofluid

Ionic ferrofluids are colloidal dispersions of magnetic nanoparticles in a liquid carrier, electrostatically stabilized thanks to the surface charges of the particles (see [15] for details on their synthesis and chemical properties). The ferrofluids used in the present work are aqueous dispersions of maghemite (γ-Fe_2O_3) nanoparticles, characterized by a mean diameter d_0 of 10 nm and a size polydispersity equal to 0.3 (both quantities are determined by a magnetization measurement). The dispersion is electrostatically stabilized thanks to the adsorption of charged citrate species at the surface of the nanoparticles. The concentration of free ions in the solvent [cit] controls the ionic strength and allows us to adjust the range of electrostatic repulsions between nanoparticles. The stability of the dispersions has been well studied in the past [16], and is shown to be related to the global interaction potential between the nanoparticles. The interaction (which can be either repulsive or attractive on average) between the particles as well as the volume fraction Φ of the particles can be controlled by a set of two parameters: the concentration of free citrate ions in the solvent [cit] and the osmotic pressure Π. This is experimentally done using an osmotic compression technique at a fixed ionic strength (see [16]). This allows us

to locate the samples in a colloidal diagram in the Π–Φ plane, presented in figure 1(a).

The colloidal phase diagram of these ionic ferrofluids presents strong analogies with that of molecular systems, namely with the existence of a liquid phase, a gas phase and a coexistence curve with a critical point on its maximum, the osmotic pressure Π being analogous to the pressure in molecular systems and the volume fraction Φ being analogous to the inverse volume $1/V$. The gas and the liquid phases are found at low osmotic pressure where the mean interparticle potential is attractive. At high osmotic pressure, the interparticle potential is repulsive and both fluid and solid phases are observed. According to these observations, the colloidal phase diagram can be split in two regions by the $\Pi V = k_B T$ line (perfect gas line indicated by the dashed line in figure 1(a), see [16]). Above this line the global interaction potential is repulsive (Yukawa like), whereas it is attractive (Lennard-Jones like) below it. Furthermore at low volume fraction, the synthesized ferrofluids are in a thermodynamic equilibrium at the end of the osmotic compression process, while at high volume fractions a colloidal glass transition is observed, leading to out-of-equilibrium, amorphous solids. Nevertheless, the same osmotic compression protocol is used for all samples; ferrofluids are kept three weeks in the bath, whatever the desired volume fraction. All the experiments are done in the week following the end of the osmotic compression process, to avoid any uncontrolled evolution of the sample.

In this work, we focus on the translational dynamics, using XPCS measurements, of a concentrated glassy sample ($\Phi = 30\%$, [cit] $= 0.03$ M) indicated by a solid star on figure 1(a). This sample is located in the repulsive part of the colloidal phase diagram.

2.2. A repulsive colloidal glass

The threshold of the dynamical arrest is located at a volume fraction that depends on the ionic strength of the dispersion. It is determined by rotational dynamics measurements, using a magneto-optical technique extensively discussed elsewhere [17–19]. This technique ensures that the selected sample presents slow dynamics (data not shown).

To certify that the concentrated ferrofluid used here is indeed a repulsive colloidal glass, we refer to the criteria of [12], where differences between glasses and gels are discussed. Although both gels and glasses are disordered systems exhibiting slow dynamics and presenting out-of-equilibrium properties, some quantitative distinctions can be pointed out:

(i) The sample used in this work, as indicated by a solid star on the colloidal diagram reported in figure 1(a), clearly belongs to the area of the phase diagram corresponding to repulsive systems. Glasses belong to this regime whereas gels usually belong to the attractive regime.

(ii) The interparticle potential in gels is attractive. It leads to the formation of large aggregates [19, 20] in the dispersion, the cooperative rearrangements of which slow down the dynamics. In repulsive colloidal glasses such structures are not observed (as seen for a hard sphere with confocal microscopy in [9]). The static structure factor $S(Q)$ (Q is the scattering vector) of gels and glasses is therefore different. Repulsive glasses have a short range order and the particles are not aggregated. This leads to a very low compressibility ($S(Q \to 0)$) and to a peak of the structure factor at a scattering vector related to the most probable distance between particles. The peak of the static structure factor in gels is shifted to higher wavevector as the close-packing of the particles and the presence of large clusters, induced by the aggregation of the particles, increase the scattered intensity at low wavevector. The structure factor is thus presenting an upturn at this large spatial scale. The static structure factor of the sample used for XPCS measurements presented in figure 1(b) clearly exhibits the aforementioned characteristics of a repulsive glass: a low compressibility ($S(Q \to 0) \sim 0.04$) and a peak at a wavevector $Q_{\max} = 5.2 \times 10^{-2}$ Å^{-1} smaller than the nanoparticle diameter.

(iii) The volume fraction threshold above which the ionic ferrofluids become amorphous increases if the ionic strength is increased [18]. The dynamical arrest of glass-forming ferrofluids is then driven by the intensity of the electrostatic repulsions.

According to all these arguments the investigated concentrated sample is a repulsive glass.

3. Slow dynamics, aging and intermittency

3.1. XPCS, time resolved correlation analysis

The translational dynamics of the concentrated sample is investigated using XPCS [21] at wavevectors covering interparticle length scales (Q-range from 0.03 to 0.045 Å^{-1}). The experiment is performed on the ID10C branch of the Troïka beamline of the European Radiation Synchrotron Facility (ESRF), allowing us to perform dynamic x-ray scattering with a collimated and partially coherent beam. The energy of the incident beam, selected thanks to a double-bounce Si(111) monochromator, is 7.03 keV, below the iron adsorption edge (7.112 keV). The speckle patterns, resulting from interferences of coherently scattered x-rays, are recorded 3.3 m from the sample on a two-dimensional charged coupled device (CCD) detector (Princeton Instruments), operating in a binning mode (both horizontal and vertical pairs of pixels are coupled, resulting in an effective pixel size of 45×45 μm^2).

A thin layer of concentrated ferrofluid is deposited on the wall of the capillary, previously filled with dodecane. It avoids evaporation that could induce a change of the volume fraction and the thickness is low enough to minimize absorption (typical thickness 10–100 μm). The age zero of the system is then defined when the sample, once placed in the capillary, is no longer subject to mechanical stress.

Time resolved speckle patterns are then recorded as a function of time t, with a time resolution of 16.43 s. The minimum lag time between frames is imposed by the acquisition time and the transfer rate of the camera onto the computer. The instantaneous degree of correlation c_I between

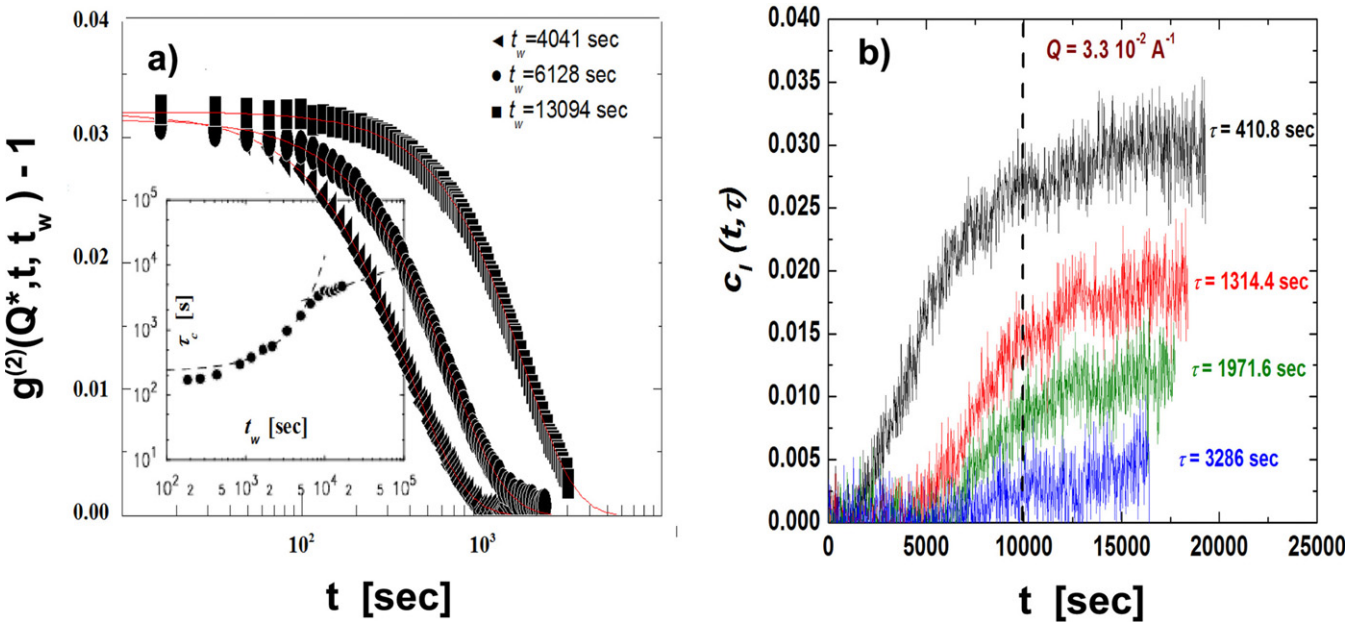

Figure 2. (a) Intensity autocorrelation function calculated at a scattering vector $Q^* = 0.044$ Å^{-1} close to $Q_{\max}$, for three different ages. From the top to the bottom, $t_w = 13\,094$, 6128 and 4041 s. Red lines are the fits of the curves using equation (3). In the inset, variation of the characteristic time τ_c at Q^* extracted from equation (3) as a function of the age t_w. (b) Degrees of correlation c_I as a function of time t for a scattering vector $Q = 0.033$ Å^{-1} and different lag times. From the top to the bottom, $\tau = 410.8$, 1314.4, 1971.6 and 3286 s. The vertical dashed line corresponds to the time above which the dynamical susceptibility χ, represented by full square symbols in figure 3(a), is calculated.

two different speckle patterns separated by a lag time τ is calculated thanks to the TRC method detailed in [22].

$$c_I(Q,t,\tau) = \frac{\langle I_p(t) I_p(t+\tau)\rangle_Q}{\langle I_p(t)\rangle_Q \langle I_p(t+\tau)\rangle_Q} - 1. \quad (1)$$

In this formula, $I_p(t)$ is the scattered intensity at pixel p and time t. $\langle \ldots \rangle_Q$ is an ensemble average over a ring of pixels defining an iso-wavevector of modulus Q.

The intensity autocorrelation functions $g^{(2)}(Q,\tau,t_w)$, as usually defined in dynamic light scattering experiments, can be computed from the time average $\langle \ldots \rangle_{t_w}$ of the degree of correlation c_I over a time interval $T_{\exp}$ around a given age t_w as:

$$g^{(2)}(Q,\tau,t_w) = \langle c_I(Q,t,\tau)\rangle_{t_w} + 1 \quad (2)$$

$g^{(2)}(Q,\tau)$ characterizes the intensity fluctuations of the interference patterns, created by coherently illuminated moving scatterers. It is therefore a signature of the dynamics of the system. For Gaussian phenomena, the intensity autocorrelation function $g^{(2)}(Q,\tau)$ is related to the dynamic structure factor $f(q,\tau)$ via the Siegert relation $g^{(2)} - 1 = \beta f^2$, where $0 < \beta < 1$ is an instrumental constant.

Note that as the function $g^{(2)}(Q,\tau,t_w) - 1 = \langle c_I(Q,t,\tau)\rangle_{t_w}$ is a time-averaged quantity, it does not allow us to study the temporal heterogeneities of the dynamics. However, it can be used to characterize the aging of the dynamics.

3.2. Slow dynamics and aging

A selection of autocorrelation functions $g^{(2)}(Q^*,\tau,t_w) - 1$ is represented in figure 2(a), at a scattering vector $Q^* = 0.044$ Å^{-1} corresponding to the peak of the scattered intensity, which is close to $Q_{\max}$, and for different ages t_w. As already discussed in [23], characteristic features of aging in glassy systems (both repulsive and attractive) are here recovered down to the nanoscale, namely:

(i) The autocorrelation functions are well modeled by compressed exponentials as indicated by the solid lines in figure 2(a),

$$g^{(2)}(Q,\tau,t_w) - 1 \propto \exp\left(-2\left(\frac{t}{\tau_c(Q,t_w)}\right)^{\beta(Q,t_w)}\right) \quad (3)$$

with $\beta \approx 1.5$ in the whole range of scattering vectors.

(ii) The characteristic time τ_c of $g^{(2)} - 1$ scales as Q^{-1} at all ages (not represented here). This observed ballistic-like scaling is a key feature of the dynamics. This surprising behavior is observed in numerous soft glasses on the micron scale, where it is related to a stress relaxation on length scales close to the interparticle distances [8].

(iii) The evolution of the characteristic time τ_c as a function of the age of the sample at the scattering vector Q^* is represented in the inset of figure 2(a). Two distinct aging regimes are observed in the whole experimental Q-range. The first one is an exponential behavior at young ages (a fast aging regime), the second is a power law, as found in spin glasses. The power law exponent is smaller than unity and a sub-aging regime is observed at all the probed length scales (a slower aging regime).

3.3. Temporal heterogeneities of the dynamics

The time resolved dynamics is investigated by means of the instantaneous degree of correlation c_I, represented on

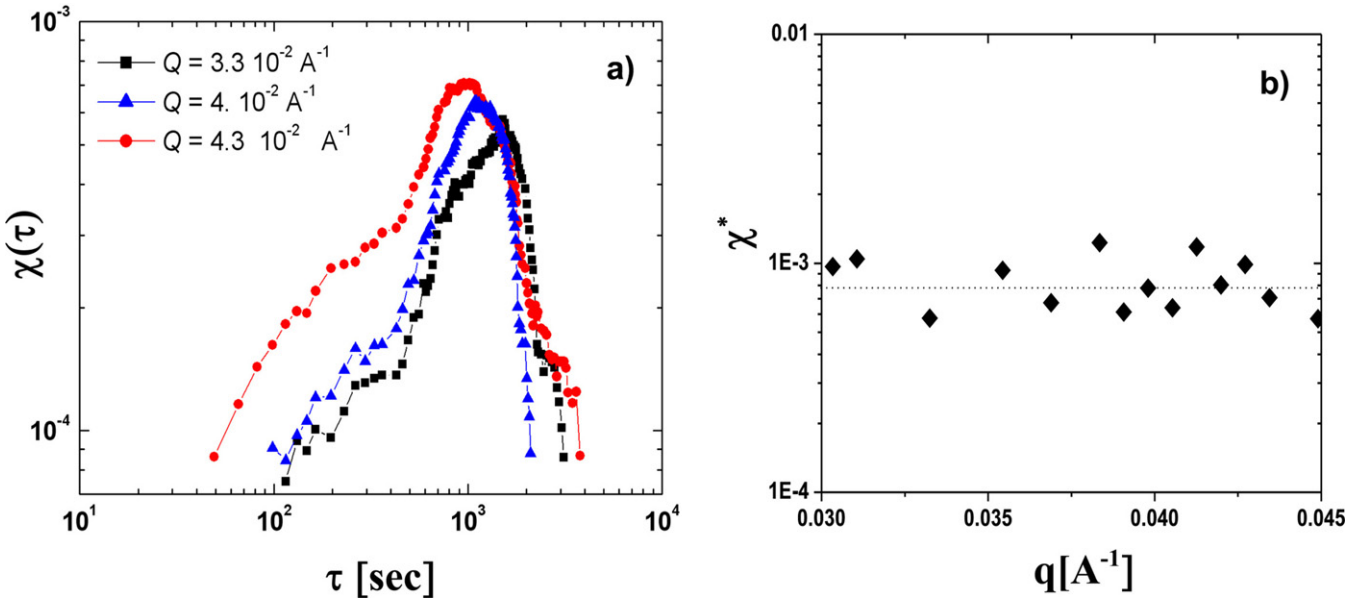

Figure 3. (a) Dynamical susceptibility, χ, as a function of τ for $Q = 0.033$ Å^{-1} (squares), $Q = 0.04$ Å^{-1} (circles) and $Q = 0.043$ Å^{-1} (triangles). (b) Maximum of the dynamical susceptibility, χ^*, as a function of Q.

figure 2(b) as a function of time t, for different time lags τ and for a $Q = 3.3 \times 10^{-2}$ Å^{-1}, close to the peak of the static structure factor. For each τ, the degree of correlation c_I is an increasing function of time, especially at short times, and is a signature of the aging processes previously described. Moreover, random spikes, which are observed along time, give a first suspicion of the intermittency of the dynamics in the concentrated ferrofluids. To prove rigorously the existence of temporal heterogeneities, the fluctuations of c_I are quantitatively analyzed, calculating its normalized temporal variance χ, which is similar to the dynamical susceptibility χ_4, usually calculated in glass formers [24]. Some precautions are taken for studying this parameter. Firstly, in order to produce significant results, the variance of the c_I is calculated in the slow (power law) aging regime, where the aging contribution can be corrected. Therefore, the variance is calculated over a time window (from $t = 10^4$ s, pointed out by a vertical dashed line in figure 2(b), until the end of the experiment) and the aging part of the dynamics is corrected by removing its linear tendency prior to the calculation of χ. Secondly, the variance is corrected for the noise contribution due to the finite number of pixels of the CCD camera (see [25] for further explanation). Lastly, to obtain the Q-dependence of χ, the variance is normalized by the squared amplitude of the relaxation of $g^{(2)} - 1$. Figure 3(a) shows χ as a function of the time lag τ and for three different Q. All the curves feature a peak, which is evidence for the heterogeneous nature of the dynamics, over the different nanometeric length scales $2\pi/Q$ investigated here. The peak position is located around the relaxation time τ_c of $g^{(2)} - 1$ (data not shown) and the peak height, called χ^* and displayed in figure 3(b), is almost constant in our experimental Q range. Therefore, the dynamical heterogeneities of the ferrofluid do not depend on the length scales in a typical range corresponding to the interparticle distance, a result in stark contrast with those obtained for two different colloidal gels, where χ^* is one order of magnitude higher and Q dependent [11, 13]. The precision of the extraction of the dynamical susceptibility is sufficient to quantify the Q-dependence of the temporal heterogeneities in our repulsive colloidal glass. However, the accuracy is not sufficient to study the probability distribution function of the dynamical fluctuations, as done in [25], and it would be useful to have quantitative information about the non-Gaussian character of the dynamics. The relatively limited extent of dynamical heterogeneities and their independence with regard to the observed spatial scales, are nevertheless interesting and should be discussed.

4. Discussion

The present measurements of the dynamical susceptibility using a TRC method are, to our knowledge, the first to be performed in a strongly repulsive colloidal glass. Indeed, following the same TRC analysis in [26], El Masri *et al* do not succeed in quantifying the spontaneous dynamical fluctuations of a hard sphere colloidal glass, the fluctuations of the c_I being too small to extract a workable variance. Nevertheless, they propose in [7] an elegant method to deduce a lower bound to the dynamical susceptibility $\chi_\Phi(\tau)$, from finite differences of the normalized intermediate scattering function, measured at nearby volume fractions Φ. They find that $\chi_\Phi(\tau)$ exhibits a peak, the maximum of which increases with increasing volume fraction close to the hard sphere glass transition. However, no length scale dependence of the maximum of χ_Φ is presented in [7].

Even in the broader range of soft glassy matter, the measurements of the dynamical susceptibility and of its Q-dependence using TRC are still scarce and difficult. The main results concern colloidal gels [11, 13], where the measurements of the dynamical susceptibility are made easier

by the origin of the dynamical fluctuations, namely the cooperative rearrangements of large clusters of particles. On the contrary, in glasses, the cooperative regions are much smaller: they contain a few particles, as revealed by numerical simulations [4]. As a result, the number of independent cooperative regions in glasses is much higher than in gels and the dynamical fluctuations, inversely proportional to the number of independent regions, are much smaller. This can explain the relatively small value of χ^* in our repulsive glass with regard to the value reported in gels [11, 13]. However, XPCS enables us to use a small scattering volume (the scattering section S is around 400 μm^2), in comparison to usual dynamical light scattering (DLS) ($S \sim 1$ cm^2). As a consequence, for a given system, the number of cooperative regions in the scattering volume is smaller in an XPCS experiment than in a DLS one. This can explain why we are able to quantify the dynamical fluctuations in our repulsive glass using XPCS, whereas it was not possible using DLS in [26].

The understanding of the Q dependence of the dynamical fluctuations in glassy systems is one of the important questions of current research into glass transitions and may help us to understand better the dynamical heterogeneities. At first view, the results concerning the Q dependence of the maximum of the dynamical susceptibility χ^* may seem controversial; for example, in [11] a linear growth of χ^* with Q was observed in a fractal gel using DLS (in the range $Qd \sim 0.004$–0.05, where d is the diameter of a particle). In a moderately attractive gel [13], a non-monotonic behavior was reported ($Qd \sim 0.5$–5). On the theoretical side, the mode coupling theory predicts a decrease of χ_Φ in the Q range close to the mean interparticle distance [27].

In [13], a model based on scaling arguments is developed by Trappe *et al* in order to rationalize these different findings. They demonstrate that a maximum of $\chi^*(Q)$ is expected at intermediate Q, at length scales close to the particle size. This result is successfully employed to understand the behavior of $\chi^*(Q)$ in gels [11, 13] and even in granular matter, where a large range of wavevectors is accessible. Indeed, in a sheared 2D granular system ($Qd \sim 0.2$–5) [14], an increase of χ^* is observed while increasing Q up to the typical grain size, followed by a decrease of the dynamical susceptibility. The maximum of χ^* is then found at a length scale smaller but close to the grain size. In colloidal glasses, no experimental results are yet available but a comparable—non-monotonic—behavior was reported, at a length scale close to the interparticle distance, in a numerical simulation of a Lennard-Jones glass former [4].

Our results thus constitute an experimental extension to the Q dependence of the dynamical susceptibility in repulsive colloidal glasses. The experimental value of χ^* is Q independent in concentrated ferrofluids, at probed length scales close to the mean particle size ($Qd \sim 2$–5). This result is indeed understandable in the framework of the model developed in [13]: close to the scattering vector corresponding to the particle size, the dynamical susceptibility exhibits a maximum. As the Q range probed in our experiment is close to this value and not very large, the value of χ^* is expected to be flat in this region. Then, as in this Q range the dynamical susceptibility is large and thanks to the experimental technique (a small beam diameter), we can explain why the dynamical fluctuations are visible in our case.

5. Conclusion

The cooperative nature of the dynamics in glasses is a key feature to understanding the slow and non-diffusive motions observed in these systems. For a particle to move, a part of its neighborhood must necessarily be engaged in this motion. A glass must then be considered as a system structured as dynamically correlated domains. When the number of these domains inside the measurement area is small, enhanced dynamical fluctuations are observed, quantified by the dynamical susceptibility χ_4.

In this paper, we have reported x-ray time resolved correlation measurements in a repulsive glass, constituted of nanosized colloids, at length scales close to the mean interparticle distance. For the first time, this method is successfully employed in a colloidal glass to probe the existence and characterize the temporal heterogeneities of its non-Gaussian dynamics. The strength of the dynamical heterogeneities is found to be Q independent at length scales close to the particle size, in good agreement with the model developed in [13]. An extension of our measurements to a broader Q range could be interesting to support the universal feature found for the length scale dependence of the dynamical susceptibility. Moreover, knowing the effects of a volume fraction variation on the dynamical fluctuations would complete our knowledge of the glass transition in concentrated ferrofluids and could bring an experimental comparison between spontaneous (χ_4) and induced (χ_Φ) dynamical fluctuations. Lastly, as the nanoparticles are highly magnetic, the effect of an external magnetic field on the dynamics is a question of interest. Under an applied magnetic field, the structure of the ferrofluid is anisotropic, at length scales close to the mean interparticle distance. This local distortion of the ferrofluid structure induces a stress at interparticle length scales which should, referring to the jamming picture of Liu and Nagel [2], be an important control parameter of the jamming transition.

Acknowledgments

The authors acknowledge P Panine of the ID02 beamline of ESRF for the small angle x-ray scattering (SAXS) measurements, D Talbot for the synthesis of ionic ferrofluids and N Malikova for careful re-reading of the manuscript.

References

[1] Gotze W, Singh A P and Voigtmann T 1999 *Phys. Rev.* E **61** 6934–48
[2] Liu A J and Nagel S 1998 *Nature* **21** 21

[3] Kirkpatrick T R and Wolynes P G 1988 *Phys. Rev.* B **36** 8552–64
[4] Lačević N, Starr F W, Schrøder T B and Glotzer S C 2003 *J. Chem. Phys.* **119** 7372–87
[5] Keys A S, Abate A, Glotzer S C and Durian D J 2007 *Nat. Phys.* **3** 260
[6] Berthier L, Biroli G, Bouchaud J-P, Kob W, Miyazaki K and Reichman D 2007 *J. Chem. Phys.* **126** 184504
[7] Berthier L, Biroli G, Bouchaud J-P, Cipelletti L, El Masri D, Ladieu F, L'Hôte D and Pierno M 2005 *Science* **310** 1797
[8] Cipelletti L and Ramos L 2005 *J. Phys.: Condens. Matter* **17** R253–85
[9] Weeks E R and Weitz D A 2002 *Phys. Rev. Lett.* **89** 095704
[10] Cipelletti L, Bissig H, Trappe V, Ballesta P and Mazoyer S 2003 *J. Phys.: Condens. Matter* **15** S257–62
[11] Duri A and Cipelletti L 2006 *Europhys. Lett.* **76** 972–8
[12] Bonn D, Tanaka H, Kellay H, Wegdam G and Meunier J 1999 *Langmuir* **15** 7534
[13] Trappe V, Pitard E, Ramos L, Robert A, Bissig H and Cipelletti L 2007 *Phys. Rev.* E **76** 051404
[14] Dauchot O, Marty G and Biroli G 2005 *Phys. Rev. Lett.* **95** 265701
[15] Berkovsky B (ed) 1994 *Magnetic Fluids and Applications Handbook* (New York: Begell House Inc.)
[16] Cousin F, Dubois E and Cabuil V 2003 *Phys. Rev.* E **68** 021405–14
[17] Wandersman E, Dupuis V, Dubois E and Perzynski R 2008 at press
[18] Mériguet G, Dubois E, Dupuis V and Perzynski R 2006 *J. Phys.: Condens. Matter* **18** 10119–31
[19] Hasmonay E, Bee A, Bacri J-C and Perzynski R 1999 *J. Phys. Chem.* B **103** 6421–8
[20] Ponton A, Bée A, Perzynski R and Talbot D 2005 *J. Phys.: Condens. Matter* **17** 821–36
[21] Robert A, Wagner J, Autenrieth T, Hartl W and Grubel G 2005 *J. Magn. Magn. Mater.* **289** 47
[22] Cipelletti L, Bissig H, Trappe V, Ballesta P and Mazoyer S 2003 *J. Phys.: Condens. Matter* **15** S257–62
[23] Robert A, Wandersman E, Dubois E, Dupuis V and Perzynski R 2006 *Europhys. Lett.* **75** 764
[24] Lačević N, Starr F W, Schrøder T B, Novikov V N and Glotzer S C 2002 *Phys. Rev.* E **66** 030101
[25] Duri A, Bissig H, Trappe V and Cipelletti L 2005 *Phys. Rev.* E **72** 051401
[26] El Masri D, Pierno M, Berthier L and Cipelletti L 2005 *J. Phys.: Condens. Matter* **17** S3543
[27] Berthier L, Biroli G, Bouchaud J-P, Kob W, Miyazaki K and Reichman D R 2006 *Preprint* cond-mat.soft/0609658v2